Paper II

Marine cold-air outbreaks in the future: an assessment of IPCC AR4 model results for the northern hemisphere

Erik W. Kolstad
Bjerknes Centre for Climate Research
Allégaten 70
5007 Bergen
Norway

Thomas J. Bracegirdle
British Antarctic Survey
Cambridge
UK

Submitted to Climate Dynamics
30 January, 2007

Abstract

For many locations around the globe some of the most severe weather is associated with outbreaks of cold air over relatively warm oceans, referred to here as marine cold-air outbreaks (MCAOs). In this study extreme MCAOs are defined as the 99^{th} quartile of the difference between the sea surface potential temperature and the potential temperature at 700 hPa. Climate model data that has been provided as part of the Intergovernmental Panel on Climate Change (IPCC) Assessment Report Four (AR4) was used to assess the models' projections for the 21^{st} century and their ability to represent the observed climatology of MCAOs.

The ensemble average of the models broadly captures the spatial distribution of the strength of MCAOs. However, there are some significant differences between the models and observations, such as excessive sea-ice extent in the Barents Sea in most of the models.

The future changes of the strength of MCAOs vary significantly between the three regions of strongest climatological values. The largest projected weakening of MCAOs is over the Labrador Sea. Over the Nordic seas the main region of strong MCAOs will move north and weaken slightly as it moves away from the warm tongue of the Gulf Stream in the Norwegian Sea. Over the Japan Sea there is projected to be only a small change to the MCAOs, with a narrow model spread. The implications of the results for mesoscale weather systems that are associated with MCAOs, namely polar lows and Arctic fronts, are discussed.

1 Introduction

A number of regions around the globe are prone to dangerous weather conditions associated with outbreaks of cold and stably stratified polar and continental air masses over relatively warm ocean surfaces. Such outbreaks, characterised by roll clouds and small-scale fronts at small fetches and deeper convection further from the coast, are referred to here as marine cold-air outbreaks (MCAOs). The strong atmospheric convection that is characteristic of MCAOs can act to enhance the intensification rate of weather systems and also contributes significantly to climatological precipitation totals. The current generation of climate models do not resolve mesoscale weather systems, such as Arctic fronts and polar lows, that are associated with MCAOs (e.g. Rasmussen and Turner 2003), thus omitting important weather phenomena from projections of future climate change.

One common feature of MCAOs, roll clouds, can have a profound impact on flux modelling of the planetary boundary layer and remain a key problem for climate models (Liu et al. 2006). Indeed this issue is not limited to low-resolution climate models, for example Pagowski and Moore (2001) found that a mesoscale model "grossly over-estimated" heat fluxes. Therefore MCAOs remain a challenging aspect of climate modelling.

Over the 21st century, projected changes to the sea-ice extent, sea surface temperature (SST) and atmospheric conditions are not uniform across the globe and will effect the strength and frequency of MCAOs to varying degrees in different regions. In addition, some studies have found that the trends of extreme cold-air outbreaks do not necessarily follow trends of mean temperature; a phenomenon known as the 'climate paradox' (Vavrus et al. 2006). Links between cold-air outbreaks and some large-scale weather patterns have also been established, demonstrating the importance of inter-annual and decadal climate variability (Vavrus et al. 2006; Dorman et al. 2004). The response of MCAOs to climate forcing therefore requires a fully coupled climate model to take into account a wide range of factors.

The importance of cold-air outbreaks to extreme weather in the Arctic can be illustrated by considering their role in the dynamics of two weather phenomena: Arctic fronts and polar lows. Arctic fronts are shallow features that define

a boundary between cold and extremely stable Arctic air masses and unstable, modified air near the warm sea surface during major cold-air outbreaks (Shapiro et al. 1989; Drue and Heinemann 2001). Although their small spatial scale precludes routine detection, shallow fronts generating strong winds are believed to occur frequently in situations with off-ice-shelf northerly flow in winter, and thus to have caused innumerable accidents at sea near the marginal ice zone (Grønås and Skeie 1999). Model simulations indicate that the corresponding large ocean-air heat fluxes and release of latent heat are important for the frontal circulation (Thompson and Burk 1991; Økland 1998; Grønås and Skeie 1999). A key dynamical feature of many Arctic fronts is that they occur when the mean flow is directed along the ice edge with the ice sheet to the right, in the opposite direction of the thermal wind. In such reverse-shear conditions (Duncan 1978; Bond and Shapiro 1991; Kolstad 2006), frontogenesis may enhance a low-level jet and near-surface wind speeds can reach hurricane force (Grønås and Skeie 1999). Greater atmospheric instability and heat fluxes over the ocean associated with stronger MCAOs will therefore, through enhanced frontogenesis, act to increase the near-surface wind speeds.

Arctic fronts can play a key role in the life cycle of intense small-scale marine cyclones known as polar lows. These potentially damaging weather systems often form in cold-air outbreaks over high-latitude oceans during the cold season months (Businger 1985), spanning November to March in the Northern Hemisphere (Lystad 1986; Noer and Ovhed 2003; Kolstad 2006). Their development is often conceptualised in two stages, where baroclinic development, often along Arctic fronts, is followed by rapid low-level cyclogenesis attributed to strong latent heat release (Nordeng 1990; Kristjansson 1990). Various theoretical explanations for their intensification have been proposed largely as a result of the wide range of observed polar low structures, which in some cases appear similar to hurricanes (Nordeng and Rasmussen 1992). Numerical experiments have shown that without the large fluxes of latent and sensible heat from the ocean to the atmosphere both baroclinic and intensely convective 'hurricane-like' numerically simulated polar lows do not attain their observed intensity (e.g. Emanuel and Rotunno 1989; Claud et al. 2004).

A large number of factors influence the strength of MCAOs over the North

Atlantic region over the 21st century. Several robust projected changes have been identified, such as sea-ice retreat (Arzel et al. 2006; Zhang and Walsh 2006), a change of the atmospheric static stability (Frierson 2006), a projected weakening of the Atlantic meridional overturning circulation (AMOC) (Gregory et al. 2005; Schmittner et al. 2005), a change of large-scale patterns; e.g. the positive trend of the North Atlantic Oscillation (NAO; Stephenson et al. 2006) and a poleward shift of the storm tracks (Yin 2005; Bengtsson et al. 2006).

The key aims of this paper are to establish the climatological characteristics of MCAOs, to evaluate the ability of climate models in simulating MCAOs and to identify and assess the projected future changes. An ensemble of Intergovernmental Panel on Climate Change (IPCC) Assessment Report Four (AR4) climate models is used as reference. The method and the model data are described in the next section, followed by the results and corresponding trends in the Northern Hemisphere. A discussion of the results follows before concluding remarks.

2 Data and methods

Only the models which provide daily temperature fields at selected pressure levels could be used in the study. This lead to the exclusion of UKMO-HADCM3, UKMO-HADGEM1, NCAR-CCSM3 and others. The models which were used, along with their average horizontal resolution in the study area and the name of their realisations under the two scenarios, are listed in Table 1.[1] All the model data was collected from ftp://ftp-esg.ucllnl.org. The 2.5 by 2.5 degree ECMWF ERA-40 reanalysis (Kållberg et al. 2004) is used as the observational reference throughout the paper. The results from the NCEP reanalysis (Kalnay et al. 1996) were practically identical and it was considered redundant to use both. To compile the model ensemble and to be able to compare the results from the models with ERA-40, the model data was interpolated onto the ERA-40 grid.

The SST is not directly available from the models. However, the 'skin temperature' (SKT) is defined on the surface and corresponds to the sea surface temperature over open water and the soil (or ice) temperature elsewhere. For our purposes,

[1] More details about the models and their full names can be found at http://www-pcmdi.llnl.gov/ipcc/about_ipcc.php.

Table 1: Abbreviations of the models that were used in the analysis, as well as their realisations and their horizontal resolution.

Model name	20C3M	SRES A1B	Lon × Lat
BCCR-BCM2.0	run1	run1	2.8° × 2.8°
CCCMA-CGCM3.1 (T63)	run1	run1	2.8° × 2.8°
CNRM-CM3	run1	run1	2.8° × 2.8°
CSIRO-MK3.0	run1, run2	run1	1.9° × 1.9°
GFDL-CM2.0	run1	run1	2.5° × 2.0°
GFDL-CM2.1	run2	run1	2.5° × 2.0°
GISS-AOM	run1	run1	4.0° × 3.0°
INGV-ECHAM4	run1	run1	1.1° × 1.1°
IPSL-CM4	run1, run2	run1	3.8° × 2.5°
MIRO3.2-HIRES	run1	run1	1.1° × 1.1°
MIRO3.2-MEDRES	run1	run1	2.8° × 2.8°
MPI-ECHAM5	run1, run4	run2, run4	1.9° × 1.9°
MRI-CGCM2.3.2a	run1	run1	2.8° × 2.8°
ERA-40	REANALYSIS	N/A	2.5° × 2.5°

this is an ideal parameter, as the SST under the ice is irrelevant to this study. Due to the nature of the skin temperature parameter, it is discontinuous at the edge of the sea-ice, where the temperature drops abruptly from a value of roughly -2°C in the ocean to several degrees below zero over the ice. To cope with this spatial irregularity, we calculated the average daily exceedance over -2°C for each grid point. A grid point with a fixed skin temperature of 8°C would then have an average exceedance of 10°C by our calculations, whereas a grid point with sea-ice throughout the year yields 0°C.

The skin temperature was only available as a monthly averaged field from the models. Because we wanted to use sea surface temperature along with daily atmospheric temperature fields, it was necessary to use an interpolation scheme to artificially increase the temporal resolution. First, for each day, the temperature was set to be the monthly mean value. Then a 31-day running-mean filter was applied at each grid point. As the ocean temperature varies on a slower time scale than that of the atmosphere, this is assumed to yield fairly realistic fields. To verify the validity of this approach, we calculated daily ERA-40 skin temperature

using the method described above with proper daily fields, and the differences were negligible for the purposes of this study (not shown).

To quantify the evolution of the MCAO indicator during a period of specified radiative forcing, we used the 20C3M scenario as the initial state of the model system. The moderate SRES A1B scenario, in which the CO_2-equivalent concentration peaks at 720 ppm in 2100 (Houghton et al. 2001), was chosen to represent the future. Because of the availability of the data, the reference periods were 1981–2000 and 2081–2100, respectively. 20 years would normally be considered insufficient to avoid oscillations due to internal variability in both models and the real atmosphere. Under the assumption that such unwanted effects are smoothed out, this is an incentive to use a model ensemble.

To assess the sensitivity to choice of reference period, the fields described above were calculated for both the 1961–1980 and the 1981–2000 ERA-40 periods. Many differences were found. In the North Atlantic, the latter period was characterised by largely positive NAO index values, and this has a strong impact in the regional circulation (e.g. Rogers 1997). In the former period, there was more sea-ice in the Greenland and Barents Seas, and the sea surface temperatures outside the east coast of North America (between latitudes 35°N and 50°N) were distinctly cooler than in the latter period (not shown). In an attempt to reduce the impact of this internal variability when comparing the model data with ERA-40, we used the 40-yr period from 1961 to 2000 as the ERA-40 reference period throughout the paper.

3 A cold-air outbreak indicator

There is no widely accepted quantitative definition of a 'cold-air outbreak'. Vavrus et al. (2006) defined cold-air outbreaks as the occurrence of two or more days during which the local mean daily surface air temperature is at least two standard deviations below the local wintertime mean temperature. However, another weather event that the term is often used to describe is the advection of cold air over a relatively warm ocean, referred to here as a marine cold-air outbreaks (MCAO). MCAOs can be readily identified on satellite imagery due to distinctive cloud characteristics such as roll clouds and cellular convection. The method used by Vavrus

et al. (2006) does not show large number of events in marine regions known to be particularly prone to MCAOs such as the Japan Sea and Norwegian Sea (Dorman et al. 2004; Grønås and Kvamstø 1995). Dorman et al. (2004) define a 'Very Cold Siberian Air Outbreak' over the Japan Sea as occurring when the 0°C isotherm is south of 40°N for more than 24 hours. In an analysis that includes the Norwegian Sea region, Bracegirdle and Gray (2007) assessed the effectiveness of various parameters for identifying polar lows that occur in MCAOs. They found that the most effective discriminator was not the atmospheric temperature or stability, but the thermodynamic disequilibrium between the ocean and atmosphere as measured by the difference between the sea surface temperature (SST) and the wet-bulb potential temperature at 700 hPa ($\theta_{w,700}$). It should be noted that the only levels available for their analysis were 900, 700 and 500 hPa. A similar approach is in fact already in practical use as Norwegian meteorologists routinely assess the difference between the SST and the temperature at the 500 hPa level as part of a polar low advanced warning service (Gunnar Noer 2005, personal communication).

In this study the MCAO indicator was based on the empirical evidence of Bracegirdle and Gray (2007), but with two minor adaptations to the parameter they chose. The first adaptation was to take into account the sea-level pressure and calculate the potential temperature of the SST (θ_{SST}) as oppose to using the SST value itself. This was motivated by the large spatial range of this study, for which different regions with large contrasts of sea level pressure are compared. The second adaptation was to use the dry potential temperature at 700 hPa (θ_{700}) rather than $\theta_{w,700}$, a choice that made a negligible difference to discriminant performance in Bracegirdle and Gray (2007). The basis for choosing the dry value here is that at warmer lower latitudes, not analysed by Bracegirdle and Gray (2007), the greater moisture capacity of the atmosphere means that the wet-bulb temperature can deviate significantly from the actual temperature. For the same reason the use of wet-bulb values at both the surface and 700 hPa was not found to be an effective indicator of MCAOs.

Here we assess projected changes of the strength of MCAOs. The extreme

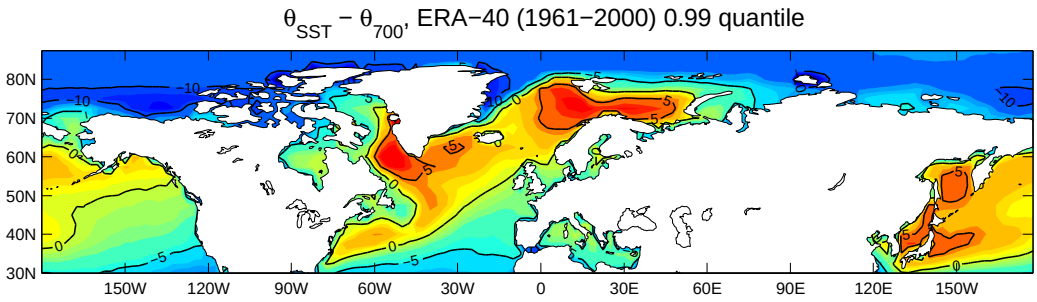

Figure 1: 0.99 quantile of the daily mean ERA-40 MCAO indicator for the period 1961–2000. The whole year is used.

events are defined as the 0.99 quantile values for all the models. The whole year is used, meaning that the quantile value is exceeded on average 3.65 times per year. Assuming that most of the extremes occur during winter, say in the course of four months, the return period of the quantile values is roughly one month.

In Figure 1, the 1961–2000 ERA-40 0.99 quantile of the MCAO indicator is shown. Three regions stand out with the strongest MCAOs.

Warm ocean currents and southwesterly winds bring warm waters to high latitudes in the Northeast Atlantic, leading to ice-free conditions all year in large parts of the Greenland, Norwegian and Barents Seas. Quantile values exceed 5°C in the Norwegian Sea region. These large values are consistent with other analyses of CAOs and associated mesoscale weather systems in that region (Lystad 1986; Noer and Ovhed 2003; Kolstad 2006).

A tongue of strong MCAO indicator values extends to the southwest of the Norwegian Sea across the North Atlantic to the eastern coast of the USA. Here, the Gulf Stream brings very warm water to relatively high latitudes. In the summer, the water in this region is frequently warm enough to sustain tropical cyclones (Jagger and Elsner 2006). During winter, outbreaks of cold continental air have been known to produce powerful low-pressure systems that have much in common with polar lows (Businger et al. 2005; Grossman and Betts 1990).

There is also a tongue of warm water extending into the Labrador Sea, where exceptionally large quantile values are found. It known that advection of cold air from Arctic Canada produces strong MCAOs in this region (Mailhot et al. 1996; Moore and Renfrew 2002; Pagowski and Moore 2001). This is an important

region for Atlantic bottom water formation (Pickart et al. 2002), therefore changes to the characteristics of MCAOs here will potentially have global implications.

The largest MCAO indicator quantile values in the North Pacific region occur around Japan and over the Sea of Okhotsk, where they match those found in the Norwegian and Labrador Seas. A range of scenarios producing cold-air outbreaks over the Japan Sea were identified by Dorman et al. (2004), who attributed the most extreme cold-air outbreaks to outbreaks of very cold Siberian air during periods of an expanded Siberian High. The Northwest Pacific is a region where both polar lows (Fu et al. 2004) and explosive extratropical cyclones (Yoshida and Asuma 2004) are known to form.

The eastern Pacific is another region where polar lows have been observed, both over the Bering Sea (Businger 1987; Businger and Baik 1991; Bresch et al. 1997) and over the Gulf of Alaska (Bond and Shapiro 1991; Douglas et al. 1991). However, the MCAO indicator values are fairly low, which is consistent with analyses of polar lows that have found convection to be more important in the intensification of Atlantic systems than those that form over the Pacific (Sardie and Warner 1983).

4 Results

4.1 Model bias and spread for 20^{th} century climatology

Figure 2 shows the average 20C3M (1981–2000) model ensemble 0.99 quantile of the MCAO indicator ($\theta_{SST} - \theta_{700}$), the inter-model standard deviation, and the bias with respect to the ERA-40 average in the period 1961–2000. Although the spatial structure is similar to the one found in Figure 1, there are some important discrepancies.

Overall, the models produce vertical gradients that are too weak in sea-ice-covered regions. The negative model bias and the spread is at its largest over the Greenland, Norwegian and Barents Seas, where the annual sea-ice distribution varies substantially (Sorteberg and Kvingedal 2006). The same negative bias-spread correlation is found over the Kara, East Siberian and Chukchi Seas along

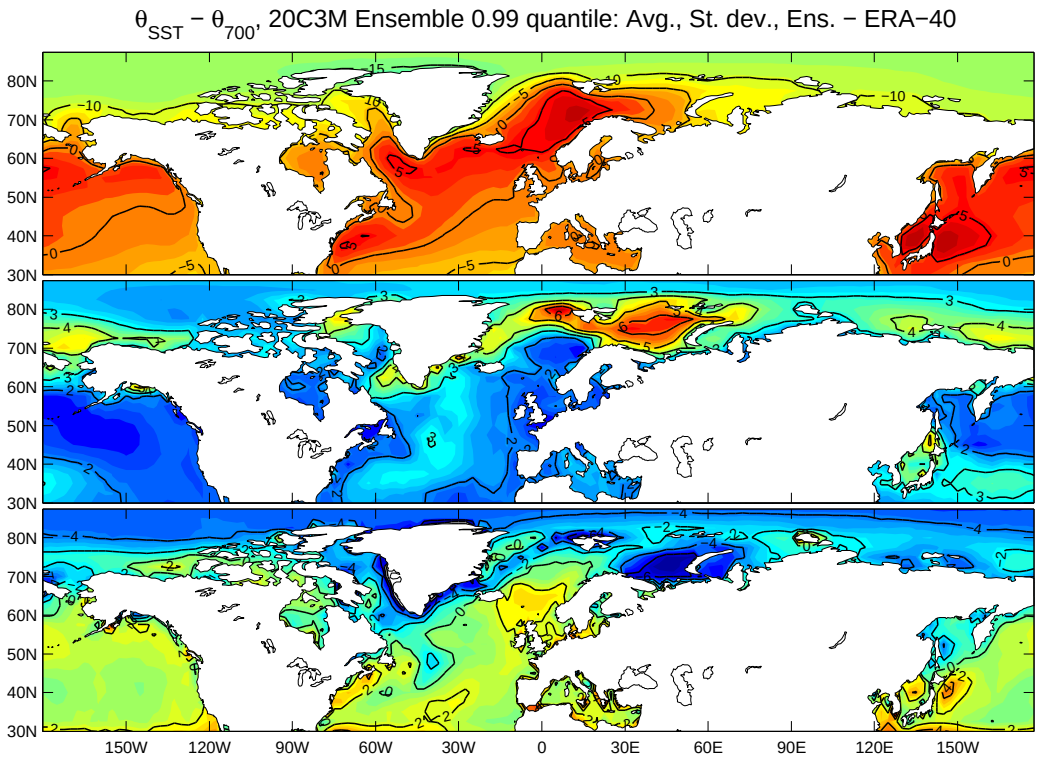

Figure 2: As Figure 1, but for the 13-model ensemble interpolated onto the ERA-40 grid (top panel); the inter-model standard deviation (middle panel); the ensemble bias with respect to ERA-40 (bottom panel).

the southern rim of the Arctic Ocean ice sheet, as well as over the Labrador Sea and Baffin Bay.

Over the open ocean the model generally overestimates the extreme values of the MCAO indicator. The largest bias and spread are found over the North and Norwegian Seas, along the east coast of North America, over the Beaufort Sea, the Gulf of Alaska and in the region around Japan.

The errors described above depend on the model representation of ocean currents and sea-ice. In Figure 3, the model skin temperature average exceedance over -2°C, as well as the spread and bias are shown. As mentioned before, there is too much ice in the Barents and Norwegian Seas. There is a similar negative bias in the Denmark Strait, although this could be due to too cold water.

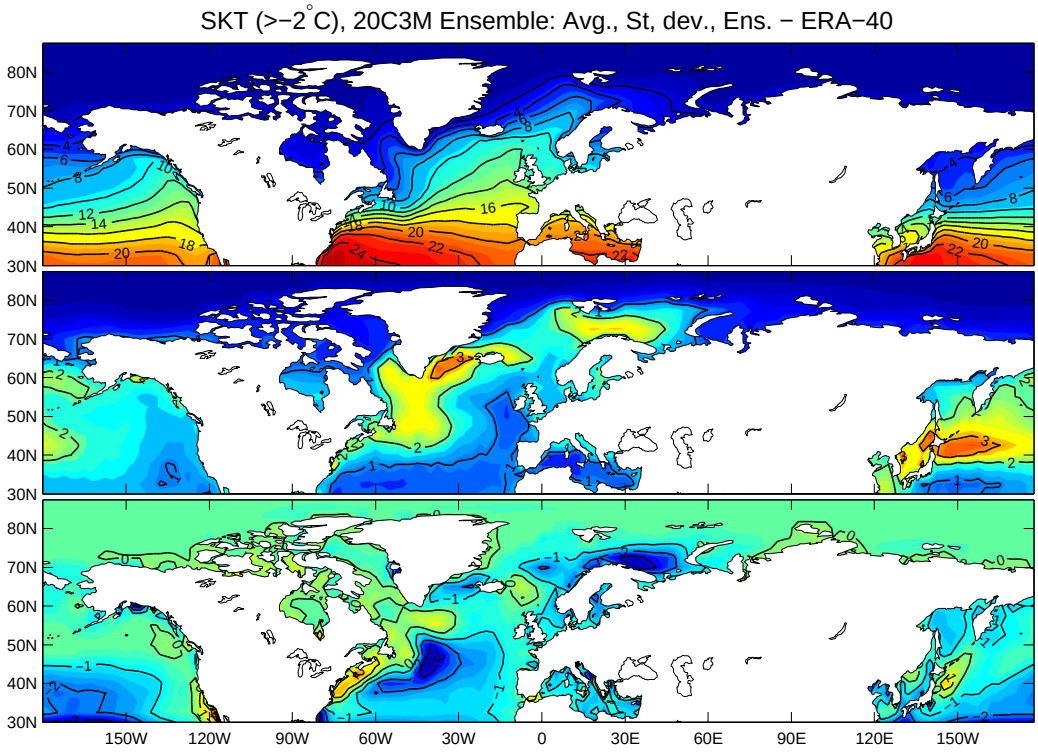

Figure 3: As Figure 2, but for the average exceedance of skin temperature over -2°C.

The coldness of the entire Northeast Atlantic suggests that warm ocean currents are unable to penetrate far enough into the Nordic Seas. Just off the east coast of North America, the ocean is too warm. Along with the cold spot futher east (which leads to a negative MCAO indicator bias near latitude 40°W), this anomaly indicates that the northward Gulf Stream passes too close to the coast. There is also a warm anomaly just south of Greenland. These large biases are likely to have a profound impact on the North Atlantic storm track in the models and are discussed later.

In the West Pacific, there is a substantial positive SST bias to the east of Japan and a negative bias in the Sea of Japan (East Sea). This is probably due to a poor representation of the cold northerly Oyashio Current and the warm southerly Kuroshio Current (e.g. Schneider et al. 2002). The model scatter is large in this region, and such errors are crucial to the validity of air-sea temperature gradients.

In some regions, such as in the Norwegian Sea, the Mediterranean and in the

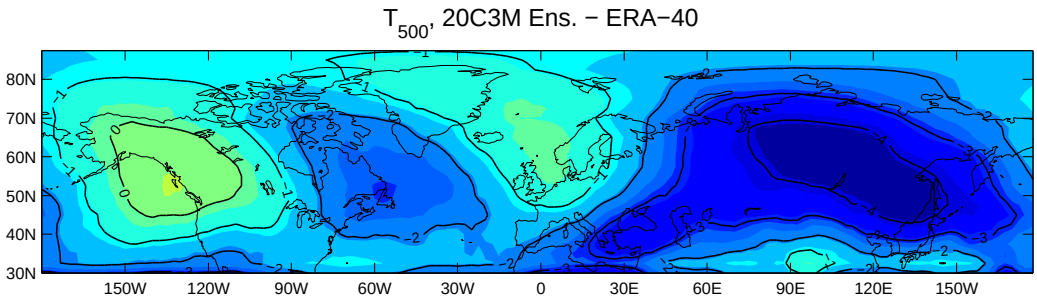

Figure 4: As the bottom panel of Figure 2, but for the air temperature at 500 hPa.

Japan Sea, there is a positive MCAO indicator bias and a negative SST bias. This is because the air masses are too cold. In Figure 4, the model ensemble bias of air temperature at 500 hPa with respect to ERA-40 is shown. Except for over the west coast of North America and the Gulf of Alaska, the ensemble is colder in the upper troposphere than ERA-40. It is clear that the amplitude of the temperature wave pattern (e.g. Thompson and Wallace 2000), with ridges over Western North America and Northwestern Europe and troughs downstream of the Rockies and over Eastern Asia, is too large in the models. At the same time, the average is too low. The negative bias is particularly strong over Siberia.

4.2 Future projections

The bias of the model ensemble is relatively strong, therefore close attention will be paid to the robustness of future changes by taking account of the inter-model spread of future changes. The changes of the MCAO indicator, the skin temperature exceeding -2°C and the 500-hPa temperature as projected by the AR4 models are shown in Figures 5, 6 and 7, respectively.

At a glance, the MCAO indicator has a negative trend over open ocean and a substantial positive trend over the sea-ice-covered Arctic region. The ocean surface warms uniformly except for a slight cooling near the southern tip of Greenland. The air at 500 hPa warms at a dramatic rate, with the smallest positive changes on the order of 3°C over the Iceland region and over the North Pacific.

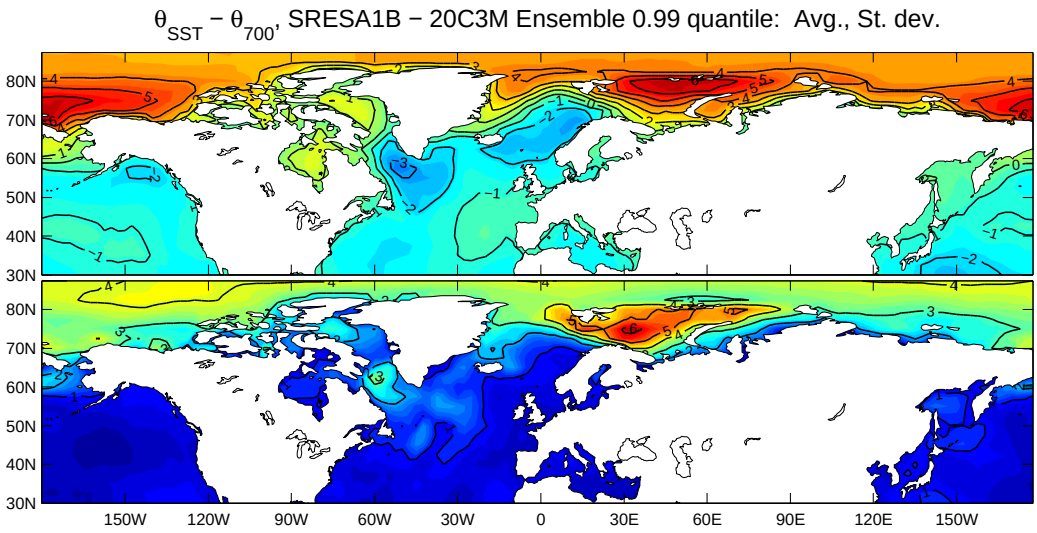

Figure 5: The difference between the ensemble MCAO indicator 0.99 quantile in the future scenario (SRES A1B) and the ensemble 20^{th} century climatology (top panel); the inter-model standard deviation (bottom panel).

However, there is also a considerable scatter of the projected changes, and each region should be carefully assessed.

4.2.1 The North Atlantic Ocean

Rapid ice retreat over the Greenland, Barents and Kara Seas leads to a large increase of the strength of MCAOs. This is most prominent to the north of the Barents Sea, with changes of over 6°C projected. Due the poor representation of the initial sea-ice, this is by far the region with the largest inter-model scatter. The changes here should therefore be treated with caution and a major improvement in models is required to reproduce current observed conditions and future changes more accurately. Much of the uncertainty in this region comes from large errors at the start of the 21^{st} century and all the models project a decrease of the sea-ice from those initial conditions. Some of the individual models project positive

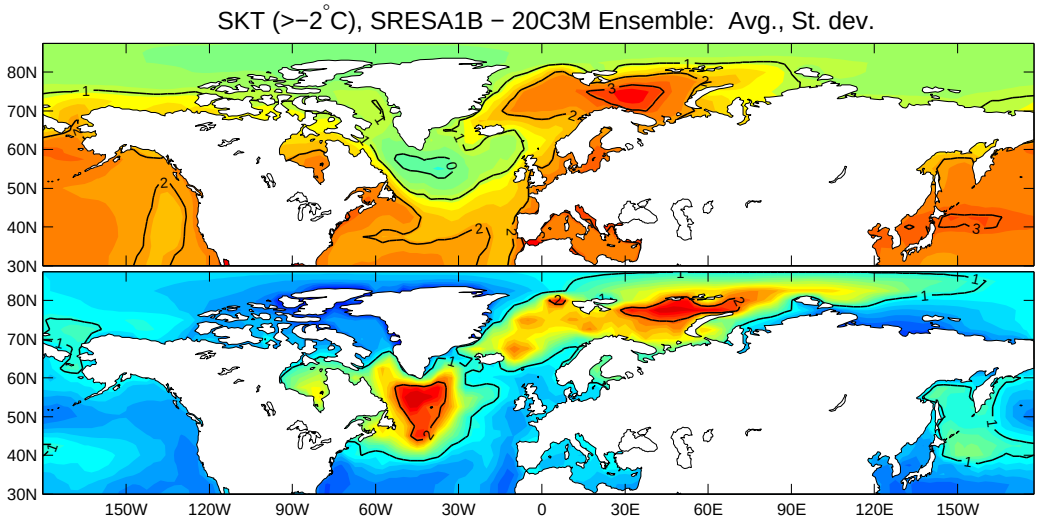

Figure 6: As Figure 5, but for the average exceedance of skin temperature over -2°C.

changes of the MCAO indicator on the order of 20°C in the Barents Sea region (individual model results are not shown).

Only three models start out with 'reasonable' sea-ice. These are: MPI-ECHAM5, which in fact has too little sea-ice at the end of the 20C3M; MRI-CGCM2.3.2a, with almost no bias; and GFDL-CM2.1, which has too much ice in the southeastern part of the Barents Sea and too little ice near Spitsbergen. They all project decreases on the order of 0-4°C in the region where they start out with open ocean, and substantial increases where they start out with sea-ice. This is a consistent signal in most of the models, even when the initial sea-ice edge is misplaced with respect to late 20^{th} century climatology. The consensus of the models is thus a robust decrease of the MCAO indicator over open ocean near the marginal ice zone, and a northward shift of the high-impact regions, following the retreating sea-ice.

The changes over the open ocean are largely negative. The most dramatic decreases are projected for the Norwegian Sea and at the entrance to the Labrador Sea south of Greenland, where the negative changes amount to more than 3°C. The simulated weakening of the AMOC in the AR4 models (Schmittner et al. 2005) is likely to be the main reason for an anomalous lack of a warming SST trend south of Greenland and the relatively weak warming of the southern Norwegian Sea (the

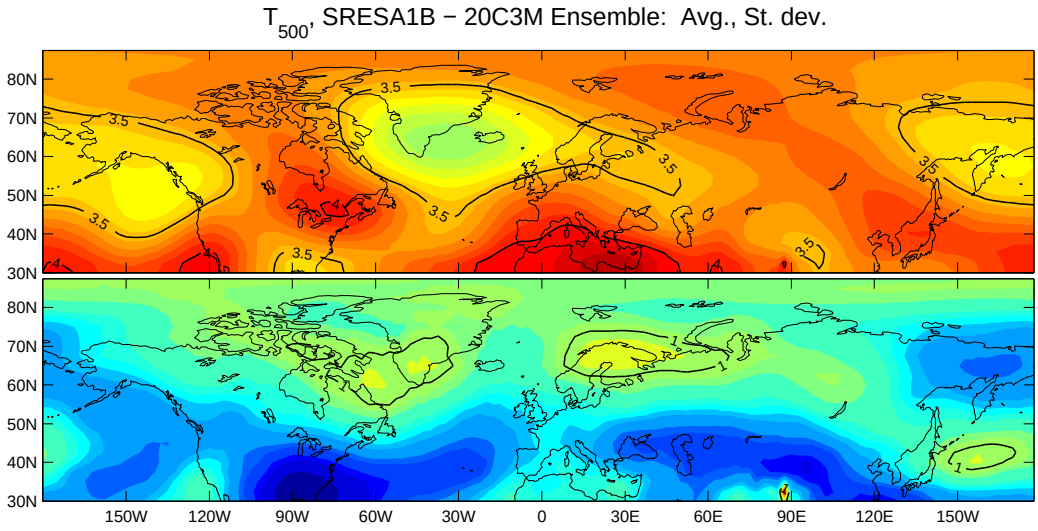

Figure 7: As Figure 5, but for the air temperature at 500 hPa.

warming in the northern part is probably due to sea-ice retreat). This contributes to a large decrease of the strength of MCAOs in the region as the atmosphere warms more than the sea surface. There is a large model spread in the region due to sea-ice extending too far south in some of the models.

Further to the south, off the eastern seaboard of the USA, the results also show decreases of around 1–2°C. Despite the strong warming projected over the north-east American continent, these changes are quite small due to the simultaneous strong warming of the SST along the coastline that is simulated in the AR4 models.

4.2.2 The Pacific Ocean

Although the model biases and the inter-model standard deviation in the West Atlantic were found to be large, the changes of the MCAO indicator in the Pacific region are smaller than those found in the Atlantic, and the model scatter is more moderate.

The smallest changes are found in the northwest, where the warming of the atmosphere is relatively weak. Over the Sea of Okhotsk the change amounts to less than 1°C. Over the Bering Sea a positive change is found, although this is most likely due to erroneous sea-ice representation during winter. In the Gulf of

Alaska, the ocean warming is somewhat less pronounced, leading to more negative changes.

The contrast to the Atlantic can largely be explained by a generally stronger warming of SSTs on the order of 2–3°C. In the Japan region, the strongest ocean warming is found exactly where the largest SST model scatter was found (Figure 3). However, this is a positive change of SST that is nearly uniform in the models, especially in the Sea of Japan (East Sea). In spite of the simultaneous warming of the atmosphere, the negative change of the MCAO indicator is limited to 1–2°C.

4.2.3 The Arctic Ocean

Large positive changes of the MCAO indicator are projected over the Arctic Ocean, especially to the northeast of the Barents Sea (as discussed above) and north of the Bering Strait (over the East Siberian and Beaufort Seas). In the latter region there is tangibly less model scatter than in the former. The models seem to agree that the ocean surface in this region will warm by 1–2°C. As this is due to retreating sea-ice, larger areas of open water will come into contact with dry, Arctic air masses (whose warming trend is fairly low compared to the rest of the northern hemisphere), and a very strong positive trend is projected for the MCAO indicator. In fact, the low model scatter suggests greater confidence in this trend than the one found near the Barents Sea. Vast new areas might be exposed to dangerous weather phenomena not previously recorded.

5 Discussion

In this study the current representation and future changes of marine cold-air outbreaks (MCAOs) have been assessed. As a result of the diversity of factors which influence them, the projected changes of MCAOs vary greatly between different regions. This will contribute to regional differences in future changes of weather associated with MCAOs.

The changes to the strength of MCAOs have important implications for changes in the activity of unresolved mesoscale weather systems. For the Atlantic region,

there are two main regions of large decrease, the Labrador Sea and Norwegian Sea. Over the marginal ice zone to the north of the Nordic seas large increases are projected.

The changes in the Labrador Sea region over the 21st century are dominated by the influence of the weakening Atlantic Meridional Overturning Circulation (AMOC; Schmittner et al. 2005). This weakens MCAOs in the region over the 21st century because the sea surface temperature (SST) remains nearly constant whilst the atmospheric temperature associated with MCAOs increases. The magnitude of the decrease of the 99th quantile of MCAOs is approximately 3°C, which will act to weaken associated polar lows and Arctic fronts.

A robust signal over the marginal ice zone in the Nordic seas is that the retreat of sea-ice produces drastic increases of the strength of MCAOs in regions of recently exposed ocean and decreases immediately south of the current marginal ice zone. Due to the large range of projected changes and initial conditions there is large uncertainty over the regional detail of the changes in the Nordic seas. Although much of the weather associated with the ice edge, such as Arctic fronts, will migrate along with the ice edge, two important observations about the projected changes were noted. Firstly, as the ice edge moves further to the north of the Nordic seas away from the warming influence of the Gulf Stream peak MCAO values will, as well as migrating, decrease in strength. This will act to reduce the intensification rate of mesoscale weather phenomena in the region of maximum MCAOs as it moves north. However, the second observation is that for polar lows, even if intensification rates are reduced, the longer life-time over the expanse of open ocean may contribute to an increased intensity of the lows before they make landfall (Emanuel and Rotunno 1989).

Other parts of the Atlantic Ocean and Mediterranean Sea show relatively small decreases of the strength of MCAOs largely due to more rapidly increasing SSTs. To the northwest of the Atlantic retreating sea-ice contributes to a slight increase of the strength of MCAOs over Hudson Bay.

In the Pacific region the most prominent location for MCAOs is along the western boundary. This shows only small decreases in strength over the 21st century compared to the decreases projected over parts of the Atlantic. This is mainly due to large SST increases, particularly in the Japan Sea region. Although

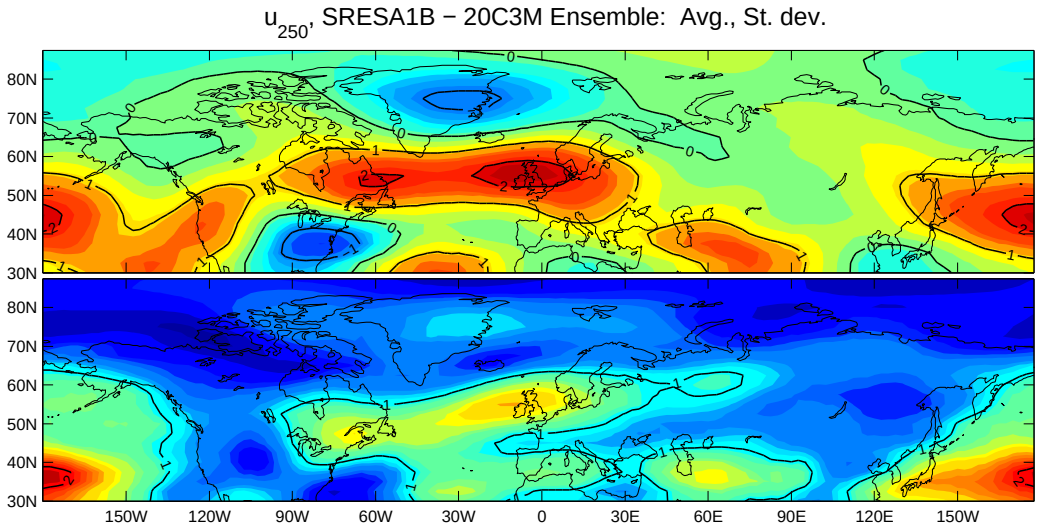

Figure 8: As Figure 5, but for the zonal wind at 250 hPa.

the slight decrease in the strength of MCAOs suggest a reduction of the severity of associated mesoscale weather systems, the coincident warmer conditions will to some extent cancel this out due to possibility for more latent heat release. Therefore the parameters assessed in this study will contribute little to changes of mesoscale weather systems in the Japan Sea region over the 21st century.

Future changes to Arctic fronts and polar lows are dependent on many factors apart from air-sea temperature difference and therefore this study should only be viewed as a first step in assessing their sensitivity to climate forcing. Other factors important to the development and maintenance of mesoscale weather phenomena include baroclinicity, forcing from upper level troughs and the ocean mixed layer depth. Many of these factors depend on the storm track, which is projected strengthen over the British Isles in the future (Bengtsson et al. 2006). This is consistent with the findings of Yin (2005), where a poleward migration of the storm track was found. Although the model ensemble used here is significantly biased with respect to the location of the upper-level jet in ERA-40 (not shown), the increase of upper-level westerly wind speed over the British Isles is a fairly robust signal (Figure 8). Also, the decrease over Greenland and the Nordic Seas is con-

sistent with the results of Bengtsson et al. (2006). One may speculate that this leads to less synoptic activity over the Nordic Seas and fewer MCAOs. Due to the large inter-model scatter, the projected strengthening of the jet over the Pacific should be treated with caution.

It is not clear how such changes in the mean flow can be related to extreme cold-air outbreaks, which are not necessarily tied to the modes of variability that are associated with storm track variability. Only through resolving mesoscale weather phenomena explicitly will their sensitivity to climate forcing be comprehensively established.

As well as their impact on weather, MCAOs are also important for air-sea interaction. Large fluxes of heat and moisture from the ocean to the atmosphere of the order of 600 Wm^{-2} can occur during MCAOs (Renfrew and Moore 1999). (In a case study of an Arctic front in the Norwegian Sea, Grønås and Skeie (1999) found that the simulated sensible heat flux exceeded 1,200 Wm^{-2}, but Pagowski and Moore (2001) have shown that heat fluxes in mesoscale models can be exaggerated.) Changes to MCAOs over the Labrador Sea will likely have the greatest impact on ocean circulation since this is a key location for bottom water formation, which contributes to the AMOC. To first order weaker MCAOs will lead to decreased heat fluxes from the ocean to the atmosphere, which will result in less bottom water formation and a further weakening of the AMOC. However, weaker mesoscale convective systems associated with the weaker MCAOs will result in less precipitation and a decrease of the freshwater input and therefore act to strengthen the AMOC. With a large modelling error associated with both of these factors (Ninomiya et al. 2006; Moore and Renfrew 2002), the role of MCAO changes in modifying ocean circulation is still uncertain and remains for future work.

6 Conclusions

The model ensemble has large biases with respect to a 40-yr ERA-40 climatology of MCAOs. The most dramatic negative biases are due to a poor representation of sea-ice in the Arctic, particularly over the Barents and Greenland Seas, but also over the Northwest Atlantic. Over open ocean, the models generally overestimate

the strength of MCAOs, mainly because the ensemble model atmosphere is too cold at 500 hPa.

In terms of future changes, a robust signal is that the strength of the MCAOs in what is now the marginal ice zone decreases substantially. At the same time, the regions with strong MCAOs moves polewards with the retreating sea-ice. An overall decrease of the MCAO indicator values is found because the atmospheric warming is more pronounced than that of the sea surface. The exception is a strong projected increase of MCAOs over newly exposed oceanic areas such as the southern rim of the Arctic Ocean.

References

Arzel O, Fichefet T, Goosse H (2006) Sea ice evolution over the 20th and 21st centuries as simulated by current AOGCMs. Ocean Modelling 12:401–415

Bengtsson L, Hodges K, Roeckner E (2006) Storm tracks and climate change. Journal Of Climate 19:3518–3543

Bond N, Shapiro M (1991) Polar Lows Over The Gulf Of Alaska In Conditions Of Reverse Shear. Monthly Weather Review 119:551–572

Bracegirdle TJ, Gray SL (2007) A new climatology of the dynamical forcing of polar lows. International Journal of Climatology submitted

Bresch JF, Reed RJ, Albright MD (1997) A polar-low development over the Bering Sea: Analysis, numerical simulation, and sensitivity experiments. Monthly Weather Review 125:3109–3130

Businger S (1985) The Synoptic Climatology Of Polar Low Outbreaks. Tellus 37A:419–432

Businger S (1987) The Synoptic Climatology Of Polar Low Outbreaks over the Gulf of Alaska and the Bering Sea. Tellus 39A:307–325

Businger S, Baik JJ (1991) An Arctic Hurricane Over The Bering Sea. Monthly Weather Review 119:2293–2322

Businger S, Graziano T, Kaplan M, Rozumalski R (2005) Cold-air cyclogenesis along the Gulf-Stream front: investigation of diabatic impacts on cyclone development, frontal structure, and track. Meteorology and Atmospheric Physics 88:65

Claud C, Heinemann G, Raustein E, McMurdie L (2004) Polar low le Cygne: Satellite observations and numerical simulations. Quarterly Journal Of The Royal Meteorological Society 130:1075–1102

Dorman CE, Beardsley RC, Dashko NA, Friehe CA, Kheilf D, Cho K, Limeburner R, Varlamov SM (2004) Winter marine atmospheric conditions over the Japan Sea. Journal Of Geophysical Research-Oceans 109:C12011

Douglas M, Fedor L, Shapiro M (1991) Polar low structure over the northern Gulf of Alaska based on research aircraft observations. Monthly Weather Review 119:32–54–

Drue C, Heinemann G (2001) Airborne investigation of arctic boundary-layer fronts over the marginal ice zone of the Davis Strait. Boundary-Layer Meteorology 101:261–292

Duncan C (1978) Baroclinic Instability In A Reversed Shear-Flow. Meteorological Magazine 107:17–23

Emanuel K, Rotunno R (1989) Polar lows as arctic hurricanes. Tellus 41A:1–17

Frierson DMW (2006) Robust increases in midlatitude static stability in simulations of global warming. Geophys Res Lett L24816

Fu G, Niino H, Kimura R, Kato T (2004) A polar low over the Japan Sea on 21 January 1997. Part I: Observational analysis. Monthly Weather Review 132:1537–1551

Gregory JM, Dixon KW, Stouffer RJ, Weaver AJ, Driesschaert E, Eby M, Fichefet T, Hasumi H, Hu A, Jungclaus JH, Kamenkovich IV, Levermann A, Montoya M, Murakami S, Nawrath S, Oka A, Sokolov AP, Thorpe RB (2005) A model intercomparison of changes in the Atlantic thermohaline circulation in response to increasing atmospheric CO2 concentration. Geophysical Research Letters 32:L12703

Grønås S, Kvamstø N (1995) Numerical Simulations Of The Synoptic Conditions And Development Of Arctic Outbreak Polar Lows. Tellus 47A:797–814

Grønås S, Skeie P (1999) A case study of strong winds at an Arctic front. Tellus 51A:865–879

Grossman RL, Betts AK (1990) Air-Sea Interaction During An Extreme Cold Air Outbreak From The Eastern Coast Of The United-States. Monthly Weather Review 118:324–342

Houghton J, Ding Y, Griggs D, Noguer M, van der Linden P, Xiaosu D (2001) *Climate Change 2001: The Scientific Basis: Contributions of Working Group I to the Third Assessment Report of the Intergovernmental Panel on Climate Change.* Cambridge University Press

Jagger TH, Elsner JB (2006) Climatology models for extreme hurricane winds near the United States. Journal Of Climate 19:3220–3236

Kållberg P, Simmons A, Uppala S, Fuentes M (2004) The ERA-40 archive. ERA-40 Project Report Series 17:31

Kalnay E, Kanamitsu M, Kistler R, Collins W, Deaven D, Gandin L, Iredell M, Saha S, White G, Woollen J, Zhu Y, Chelliah M, Ebisuzaki W, Higgins W, Janowiak J, Mo K, Ropelewski C, Wang J, Leetmaa A, Reynolds R, Jenne R, Joseph D (1996) The NCEP/NCAR 40-year reanalysis project. Bulletin Of The American Meteorological Society 77:437–471

Kolstad E (2006) A new climatology of favourable conditions for reverse-shear polar lows. Tellus 58A:344–354

Kristjansson J (1990) Model simulations of an intense meso-beta scale cyclone. The role of condensation parameterization. Tellus 42A:78–91

Liu A, Moore G, Tsuboki K, Renfrew I (2006) The effect of the sea-ice zone on the development of boundary-layer roll clouds during cold air outbreaks. Boundary-Layer Meteorology 118:557–581

Lystad M (1986) Polar lows project; Final report: polar lows in the Norwegian, Greenland and Barents Sea

Mailhot J, Hanley D, Bilodeau B, Hertzman O (1996) A numerical case study of a polar low in the Labrador Sea. Tellus 48A:383–402

Moore G, Renfrew I (2002) An assessment of the surface turbulent heat fluxes from the NCEP-NCAR reanalysis over the western boundary currents. Journal of Climate 15:2020–2037

Ninomiya K, Nishimura T, Suzuki T, Matsumura S (2006) Polar-Air Outbreak and Air-Mass Transformation over the East Coast of Asia as Simulated by an AGCM. Journal of the Meteorological Society of Japan 84:47–68

Noer G, Ovhed M (2003) Forecasting of polar lows in the Norwegian and the Barents Sea. In: *9th meeting of the EGS Polar Lows Working Group*, Cambridge, UK

Nordeng T (1990) A model-based diagnostic study of the development and maintenance mechanisms of two polar lows. Tellus 42A:92–108

Nordeng T, Rasmussen E (1992) A Most Beautiful Polar Low - A Case-Study Of A Polar Low Development In The Bear-Island Region. Tellus Series A-Dynamic Meteorology And Oceanography 44A:81–99

Økland H (1998) Modification of frontal circulations by surface heat flux. Tellus 50A:211–218

Pagowski M, Moore G (2001) A numerical study of an extreme cold-air outbreak over the Labrador Sea: Sea ice, air-sea interaction, and development of polar lows. Monthly Weather Review 129:47–72

Pickart RS, Torres DJ, Clarke RA (2002) Hydrography of the Labrador Sea during Active Convection. Journal of Physical Oceanography 32:428–457

Rasmussen E, Turner J (2003) *Polar Lows*. Cambridge University Press, Cambridge

Renfrew IA, Moore G (1999) An extreme cold-air outbreak over the Labrador Sea: Roll vortices and air-sea interaction. Monthly Weather Review 127:2379–2394

Rogers J (1997) North Atlantic storm track variability and its association to the north Atlantic oscillation and climate variability of northern Europe. Journal of Climate 10:1635–1647

Sardie JM, Warner TT (1983) On The Mechanism For The Development Of Polar Lows. Journal Of The Atmospheric Sciences 40:869–881

Schmittner A, Latif M, Schneider B (2005) Model projections of the North Atlantic thermohaline circulation for the 21st century assessed by observations. Geophysical Research Letters 32:L23710

Schneider N, Miller AJ, Pierce DW (2002) Anatomy of North Pacific decadal variability. Journal Of Climate 15:586–605

Shapiro M, Hampel T, Fedor L (1989) Research aircraft observations of an arctic front over the Barents Seas. In: *Polar and Arctic Lows*, A Deepak, Hampton, VA, 279–89

Sorteberg A, Kvingedal B (2006) Atmospheric forcing on the Barents Sea winter ice extent. Journal Of Climate 19:4772–4784

Stephenson DB, Pavan V, Collins M, Junge MM, Quadrelli R, Groups PCM (2006) North Atlantic Oscillation response to transient greenhouse gas forcing and the impact on European winter climate: a CMIP2 multi-model assessment. Climate Dynamics V27:401–420

Thompson DWJ, Wallace JM (2000) Annular Modes in the Extratropical Circulation. Part I: Month-to-Month Variability*. Journal of Climate 13:1000–1016

Thompson W, Burk S (1991) An investigation of an Arctic front with a vertically nested mesoscale model. Monthly Weather Review 119:233–261–

Vavrus S, Walsh JE, Chapman WL, Portis D (2006) The behavior of extreme cold air outbreaks under greenhouse warming. International Journal Of Climatology 26:1133–1147

Yin JH (2005) A consistent poleward shift of the storm tracks in simulations of 21st century climate. Geophysical Research Letters 32:L18701

Yoshida A, Asuma Y (2004) Structures and Environment of Explosively Developing Extratropical Cyclones in the Northwestern Pacific Region. Monthly Weather Review 132:1121–1142

Zhang XD, Walsh JE (2006) Toward a seasonally ice-covered Arctic Ocean: Scenarios from the IPCC AR4 model simulations. Journal Of Climate 19:1730–1747